Design of a Soft Robophysical Earthworm Model

Yasemin O. Aydin, Jennifer L. Molnar (*IEEE Student Member*), Daniel I. Goldman, and
Frank L. Hammond III (*IEEE Member*)

Abstract—**Soft-bodied organisms accomplish their locomotor tasks in complex environments based primarily on changes in the dimensions of their body segments. Inspired by the morphology and behavior of the earthworm, we designed a multi-segmented soft worm robot and tested its performance experimentally through three locomotion tests: forward/backward motion, turning motion and sideways motion on a hard surface**.

I. INTRODUCTION

Peristaltic robots take inspiration from biological models such as the earthworm (*Lumbricus terrestris*), which produces forward motion through wave-like patterns of contraction and extension that progress from anterior to posterior [1, 2, 3, 4]. The earthworm accomplishes this through contraction of circular and longitudinal muscles, which act on its constant-volume, hydrostatic segments to alternately produce radial expansion and longitudinal compression (anchoring) or radial contraction and longitudinal extension (forward movement).

Peristalsis is not unique to the earthworm, and other soft-bodied animals such as caterpillars, sea cucumbers, and snails exhibit peristaltic mechanisms that utilize unsegmented hydrostatic skeletons, waves that move from posterior to anterior, waves that are concentrated into a flattened pedal "foot," and muscular structures that are predisposed to undulating rather than laterally symmetric waves [5]. However, the earthworm provides an excellent example of a soft-bodied animal which can locomote both aboveground, belowground, and on marginal terrains, and has often been the inspiration for peristaltic robots.

Two primary types of peristaltic robots exist in literature: mesh robots and soft pneumatically-actuated robots. Seok et al built a four-segment mesh robot surrounded by NiTi memory wire; electrically-induced heating caused the segments to contract sequentially, inducing peristaltic forward motion [6]. Longitudinal actuators on either side of the robot could be activated to induce sideways curvature in the robot, permitting steering. Boxerbaum et al took a similar mesh-frame approach but created a continuously deformable (rather than discretely-segmented) robot [7]. Deviating from a legless design, Trimmer built a combination pneumatic- and memory-wire-actuated robot with "prolegs," a design inspired by the *Manduca sexta* caterpillar [8, 9]. Gilbertson devised a purely pneumatic soft robot which deviated even farther from the original earthworm peristaltic model, utilizing a helical
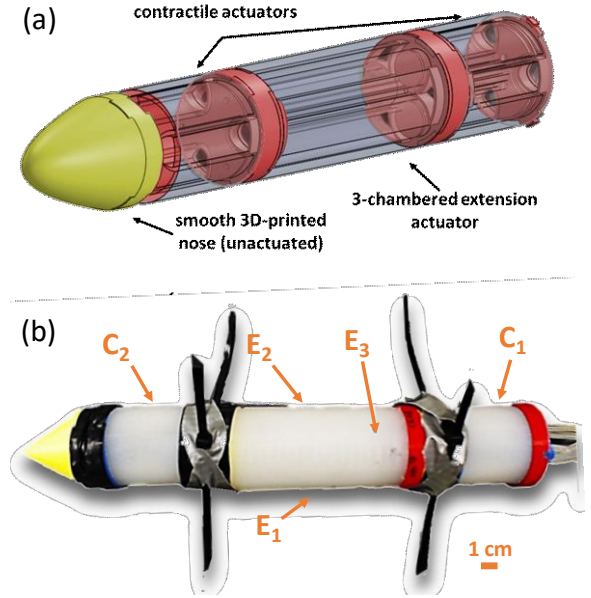
Figure 1. (a) CAD model of fully assembled robot, with silicone bodies made transparent for easier visualization of the intermediate connectors. Tubes routed through proximal actuators can be redirected into distal chambers within the hollow space inside the connectors. (b) Photo of robot after construction. "C" represents a contractile (radially expanding) actuator, "E" indicates a (longitudinally) extensile actuator, three of which together make up the central bending/extending segment.

shape designed for tube traversal [10]. This robot braced itself against the side of a tube without filling it completely, allowing it to anchor and travel without fully occluding flow.

These robots show that peristaltic motion is fruitful for aboveground and through-tunnel traversal, but earthworms are also capable of other forms of motion (e.g. burrowing underground). This is a form of peristalsis that has not been imitated, nor is it yet well understood. In this paper, we aim to construct a soft, pneumatically-actuated robot to act as a simplified robophysical model of an earthworm. The *robophysical* approach takes advantage of the physicality of a robot model to uncover principles of locomotion within environments that would be difficult to simulate theoretically [11]. The robot is not intended to faithfully replicate the earthworm in every regard; instead, it is intentionally simplified. The robophysical model provides a platform for isolating and testing basic locomotor hypotheses, including mechanisms for effective peristaltic motion above (and eventually below) ground and the contributions of environmental parameters to effective motion.

II. OBJECTIVES

Our goal is to develop a steerable, earthworm-inspired robot with fluidic (pneumatic) actuation and a minimal set of

segments, for exploring principles of peristaltic motion. A pneumatic design is selected for its similarity to the biological hydrostatic skeleton, while the minimal set of segments is used as a starting point for exploring factors that affect the effectiveness of peristaltic gaits. The design and fabrication of this robot is detailed in Section III. Section IV describes the robot's locomotive capabilities on a flat surface, including forward/reverse peristalsis and steering. In Section V, gait quality is discussed, and Section VI contains insights for future robot designs and gait experiments.

III. DESIGN AND FABRICATION OF THE SOFT EARTHWORM ROBOT

The peristaltic motion of the earthworm depends on its ability to anchor itself alternately at either end [11]. A radially-expanding actuator at each end of the robot provides this anchoring mechanism, while a longitudinally-expanding actuator serves as the connection between the two (Figure 1). To permit steering, that central actuator contains three cylindrical extension chambers, which allows it to operate as either an extensile or a bending actuator, depending on the number of chambers which are pressurized simultaneously.

A. Central Extensile/Bending Actuator

The authors assume that the reader is familiar with the general silicone-casting procedure outlined by the Soft Robotics Toolkit [12]. The process for constructing the extensile/bending segment was modified from the fiber-reinforced actuator construction process described on that website, with inspiration taken from the four-chambered manipulator developed by Marchese and Rus [13].

The three 10-cm cylindrical extensile chambers, with outer diameter of 17 mm and thickness of 2 mm, were cast with DragonSkin10 silicone (Smooth-On, Inc.) in 3D-printed molds (uPrint SE Plus, Stratasys, Ltd.) around cylindrical plugs. The mold produced helical groves on the outer surface of the silicone at 5 mm intervals, which served as guides for a nylon thread that was wrapped around the cylinders in double-helical fashion (see Figure 2. Extensile/bending actuator body, with three independent cylindrical extension chambers. Nylon thread was wrapped at a pitch of 5mm (shown on only one chamber for clarity) to constrain
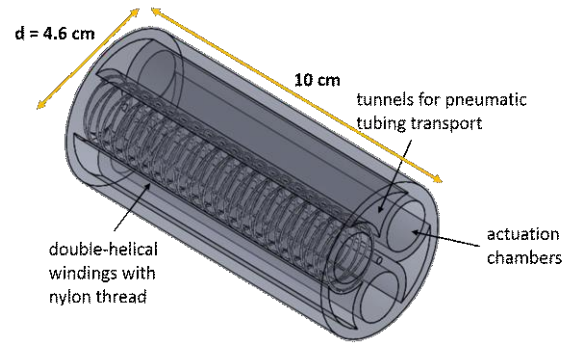

Figure 2. Extensile/bending actuator body, with three independent cylindrical extension chambers. Nylon thread was wrapped at a pitch of 5mm (shown on only one chamber for clarity) to constrain expansion to the longitudinal axis. By actuating individual chambers, bending can be achieved; the angle of bending can be modulated by varying the pressure between chambers. When all three chambers are pressurized equally, the actuator extends without bending.

expansion to the longitudinal axis. By actuating individual chambers, bending can be achieved; the angle of bending can be modulated by varying the pressure between chambers. When all three chambers are pressurized equally, the actuator extends without bending.). Three such chambers were then inserted into a larger encapsulating mold and Ecoflex-50 (Smooth-On, Inc.) was poured in, to encapsulate the nylon wrapping and connect the three chambers without increasing the stiffness of the actuator or making it difficult to pressurize. Space between the chambers was kept open for later tubing and sensor routing through the use of additional 3D-printed plugs positioned between the cylindrical chambers. The completed actuator was 10.0 cm long by 4.6 cm in diameter.

B. Radially-expanding actuators

Pulling from the standard repertoire of actuators in the Soft Robotics Toolkit [12], the initial choice for the radially-expanding actuators was a pneumatic artificial muscle (PAM) with Flexo PET Overexpanded Braided Sleeving (TechFlex) as the constraining mesh. However, despite its high stretch when not encapsulated by silicone, in the completed actuator, the mesh constrained the radial expansion more than was desirable for effective anchoring. The final actuator design consisted of a single chamber 3 mm thick with a 4.6 cm outer diameter. No fibers were embedded at its outer surface, to enable maximal radial expansion, while longitudinal extension was prevented via S-glass-reinforced tunnels that extended from one end to the other, as shown in Figure 3. The S-glass also served to prevent the collapse of the tunnels, which were used to route pneumatic tubing through the proximal actuators to connect to more distal ones.

Construction of the actuators was done by first imbuing S-glass fabric with silicone. The fabric was placed on top of a transparency and silicone was poured over top of it. A second transparency was then placed on top, the layers were smoothed with a rolling pin, and the silicone was allowed to dry. This silicone-embedded S-glass was cut into the appropriate size to fit around the interior edge of the tunnel, and pressed into the sides of a removable plug. The plug was inserted into the main mold, which was filled with
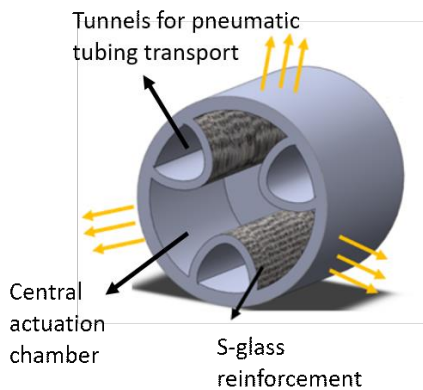

Figure 3. Radially-expanding actuator body, with the fiber reinforcement only provided along the interior wall of the pneumatic tubing tunnels. Yellow arrows show the extension direction of the actuator.
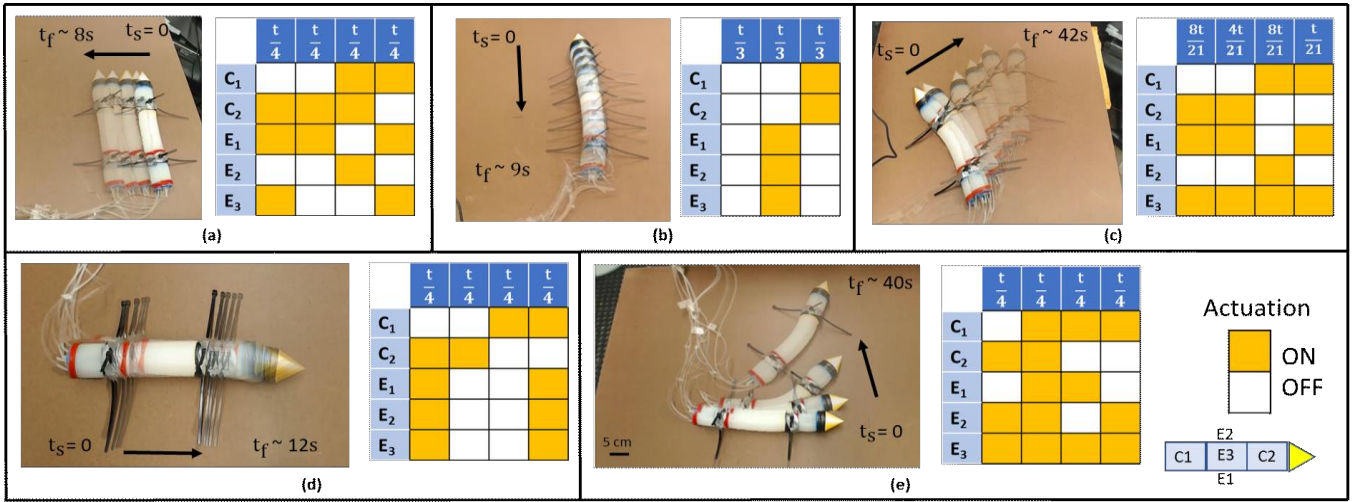
Figure 4. Motion sequences showing the Wormbot gaits on a flat particleboard. The activation pattern of the segments during a cycle is given at the right. C_1: front, C_2: back contractile actuator, E_1: left, E_2: right and E_3 is the top inner segment of the extensile actuator given in Figure 1-b. Yellow color means that the corresponding actuator is activated at that time interval and t is the full gait cycle duration, t_s is the start time and t_f is the final time. (a) Left sideways motion (b) Backward motion (c) Clockwise turn while moving forward (d) Forward motion (e) Counterclockwise turn.

DragonSkin10, completing the actuator body in a single casting.

C. Pneumatic routing and connections

The actuator ends were finished with plastic end caps 3D-printed from the same uPrint Stratasys printer. At the closed end of the actuator body, a thin flat plate placed against the interior wall provided a rigid structure for securing the end cap via screws. The end of the chamber was then sealed with a thin layer of Ecoflex-50. A 3D-printed reinforcement ring was placed around the silicone and press-fit onto the edge of the connector; this ring reduces expansion of the silicone at the connector interface, which is an area vulnerable to leakage.

After securing the closed-off end, the open end was fitted with a ridged 3D-printed cap and glued there with a silicone-based adhesive (Sil-Poxy, Smooth-On, Inc.). Silicone-rubber tubing was inserted through holes in the end cap and similarly secured with Sil-Poxy glue. To finalize the seal, Ecoflex50 silicone was injected via syringe into the base of the chamber, with care taken not to allow silicone to flow into the pneumatic tubing. The hole created by the syringe self-sealed, completing the actuator.

Figure 5. Pneumatic control board that includes solenoid valves, high speed MOSFETs, pressure sensors and an Arduino Mega 2560 controller.

The end pieces were designed to press-fit together with spacers to allow pneumatic tubes to be routed from open tunnels into their destination chambers (Figure 1). This modular construction allows for a minimalist design for proof-of-concept gait, but also permits easy changes to the number or types of actuators used if different combinations prove useful for future tasks.

IV. EXPERIMENTAL PROCEDURE

The robot was pneumatically actuated using an open source design for a fluidics control board taken from the Soft Robotics Toolkit [12]. The board was controlled through an Arduino Mega 2560, with five solenoid valves, power regulators and MOSFET power switches to provide pressurization for five independent actuation chambers (Figure 5). A 70 KPa air source provided pressurized air to the system, and the pneumatic pressure of each segment was adjusted by pulse-width modulation of the solenoid valves.

The robot's performance was tested on flat particleboard and recorded using a webcam. Low-friction plastic rods in the form of zip-ties were attached to the robot's sides to prevent rolling. Figure 4 shows the activation patterns of each gait we tested, where time intervals progress from left to right and yellow boxes indicate chamber activation. The most bioinspired gait was forward peristaltic motion, using front and rear contractile actuators to anchor each side alternately while the central section expanded and contracted to push the robot forward. Unfortunately, fabrication inconsistencies led the contractile actuators to expand unequally, so that the rear actuator had trouble anchoring. For this reason, backwards peristalsis turned out to be more effective than forward peristaltic motion, and also required a modification to the gait pattern to accommodate the difference in deflation rate between the front and rear actuators.

Additional attempted gaits included turning (clockwise and counter-clockwise) and sideways motion. Sidewinding is not observed in earthworms, but the sequence of actuators used
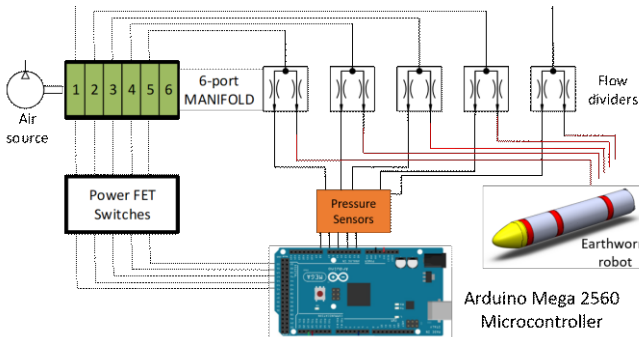
for normal peristalsis proved capable of generating this motion as well. To creep by means of the sideways gait, the robot anchors both the front and rear actuators (C_1 and C_2) simultaneously, then raises the central part of its body from the ground by inflating the middle extensile segment (E_3). It then inflates the segment on the side matching the direction of motion, causing it to bend and then fall in that direction. By successively inflating different regions of the body, the robot anchors either the outer or central part of its body and moves the free part(s) sideways, without ever having to slide. This efficient use of cleanly anchored/unanchored actuators produced the fastest gait of all the gaits attempted, despite being the one least correspondent to the biological target. However, this gait becomes unpredictable if the robot is allowed to roll; un-earthworm-like plastic zip-tie extensions were used to prevent such motion.

V. RESULTS

Behavior for each of the actuation patterns can be seen in Figure 4. The robot was able to move about 3.6±0.3 mm/cycle with forward peristalsis and 11.0±1.6 mm/cycle in reverse, 14.8±0.3 mm/cycle with sideways gait. It can turn about 4±0.2 deg/cycle with clockwise and counterclockwise gaits.

There are two types of steering motion: rotation in place, and turning while moving forward. The former is much like forward peristalsis in that it begins by anchoring the back actuator and extending the central one; to induce turning, this is followed by deflating one of the chambers to cause a bending motion before the front actuator is anchored and the rear one releases. For steering while moving forward, the movement pattern is a hybrid of forward peristalsis and sidewinding gaits. The robot extends forward as per normal peristalsis, then induces a sideways bend in the direction of rotation before anchoring the central actuator for the sidewinding part of the gait. The inflation of the central chamber is exaggerated so that it forms a smooth, round contact surface with the ground; when the front and rear actuators are raised, the added weight of the pneumatic tubing permits the robot to rock backward slightly and anchor closer to the rear end of the robot. This allows the front actuator to raise more than the rear one, so that it travels farther before landing. Thus, a small rotation occurs during side-winding, allowing steering to occur in conjunction with forward movement.

Regardless of the gait chosen, the ability of the robot to cleanly and fully switch between anchoring and sliding for the radially-expansive actuators appears to be the most important part of the robot's locomotion. For instance, the lower inflation of the rear actuator limited its anchoring ability, which slowed forward peristalsis to a third of the speed of the reverse gait. The importance of reducing friction during sliding was made most obvious by the success of the sidewinding gait, which had no sliding phase. Straight or rotational peristaltic motion, on the other hand, relied on sliding either the forward or rear actuator during the gait cycle, which necessarily lost efficiency due to friction as well as to the inability of the anchoring side to stay completely secure while the free end moved in the direction of locomotion.

VI. FUTURE WORK

The three-segment Wormbot contains the basic features necessary for peristaltic locomotion with some steering capability, as demonstrated by the five flat-surface gaits above. For more efficient and versatile motion, further work must be done to determine effective ways of increasing friction when anchoring is desired and decreasing it for the sliding phase of the gait. Robotic versions of earthworm setae are one avenue which could be pursued; weight maneuvering and increasing the maximum radius of expansion for the anchoring actuator are others. Tests must also be conducted over different types of substrates to determine effectiveness on sloped, textured, or granular material. Eventually, methods of anchoring that are effective within a substrate (i.e. underground) must be established, and those principles compared with earthworm observations and experiments to determine if those principles are relevant to both the biological and robotic domains.

The extensile actuators were based on prior designs and functioned desirably, but the anchoring actuators could be developed further in future designs. For instance, points at the junction between the stiff S-glass-reinforced tunnels and the flexible exterior of the silicone are currently vulnerable to leakage, but could be reinforced by modifying the mold to have thicker silicone near that boundary. A consistent radius of expansion can be achieved by ensuring that inner molds use guide posts to remain centered within outer molds while curing.

Shape monitoring can be achieved by the integration of optical sensors [14], which will allow for closed-loop motion control and potentially allow the robot to intelligently compensate for rotation. This will be important when the robot moves underground, where the plastic extensions that prevented rolling on a flat surface will no longer be usable or effective. Integrating such sensors may also allow the Wormbot to sense contact pressures with surrounding dirt and choose to navigate through areas that match its preferred stiffness properties. It can also adapt its gait to environmental circumstances and cross the obstacles.

REFERENCES

[1]   R. M. Alexander, Locomotion of Animals., New York:: Chapman & Hall, 1982.

[2]   R. M. Alexander, Animal Mechanics. Second edition, Oxford: Blackwell Scientific Publications., 1983.

[3]   E. Trueman, The Locomotion of Soft Bodied Animals, New York: American Elsevier Publishing Company, Inc., 1975.

[4]   J. Gray, Animal Locomotion, London, 1968.

[5]   H. Y. Elder, "Peristaltic Mechanisms," *Society for Experimental Biology, Seminar Series ,* vol. 5, pp. 71-92, 1980.

[6]   S. Seok, C. D. Onal, K.-J. Cho, R. J. Wood, D. Rus and S. Kim, "Meshworm: A Peristaltic Soft Robot With Antagonistic Nickel Titanium Coil Actuators," *IEEEASME Trans. Mechatron.,* vol. 18, no. 5, p. 1485–1497, Oct. 2013..

[7]   A. S. Boxerbaum, K. M. Shaw, H. J. Chiel and R. D. Quinn, "Continuous wave peristaltic motion in a robot," *The International Journal of Robotics Research,* vol. 31, no. 3, pp. 302-318, March 2012.

[8]   B. A. Trimmer, A. E. Takesian and B. M. Sweet, "Caterpillar locomotion: A new model for soft-bodied climbing and burrowing robots," in *7th International Symposium on Technology and the Mine Problem*, Monterey, CA, May 2006.

[9]   T. Umedachi, V. Vikas and B. A. Trimmer, "Softworms : The Design and Control of Non-Pneumatic, 3D-Printed, Deformable Robots," *Bioinspiration & Biomimetics,* vol. 11, no. 2, 2016.

[10] M. D. Gilbertson, G. McDonald, G. Korinek, J. D. Van de Ven and T. M. Kowalewski, "Serially Actuated Locomotion for Soft Robots in Tube-Like Environments," *IEEE Robotics and Automation Letters,* vol. 2, no. 2, pp. 1140-1147, April 2017.

[11] J. Aguilar, T. Zhang, F. Qian, M. Kingsbury, B. McInroe, N. Mazouchova, C. Li, R. Maladen, C. Gong, M. Travers, R. L. Hatton, H. Choset, P. B. Umbanhowar and D. Goldman, "A review on locomotion robophysics: the study of movement at the intersection of robotics, soft matter and dynamical systems,," *Reports on Progress in Physics,* vol. 110001 , p. 79 , 2016.

[12] Y. Tanaka, K. Ito, T. Nakagaki and R. Kobayashi, "Mechanics of Peristaltic Locomotion and Role of Anchoring," *Journal of the Royal Society Interface,* vol. 9, no. 67, p. 222–33, 2012.

[13] D. P. Holland, E. J. Park, P. Polygerinos, G. J. Bennett and C. J. Walsh, "The soft robotics toolkit: shared resources for research and design," *Soft Robotics,* vol. 1, no. 3, pp. 224-230, 2014.

[14] A. D. Marchese and D. Rus, "Design, Kinematics, and Control of a Soft Spatial Fluidic Elastomer Manipulator," *The International Journal of Robotics Research ,* vol. 35, no. 7 , p. 840–69, 2016.

[15] F. Caralt, J. Molnar, T. Cahoon, J. Stingel and F. L. Hammond, "Diffusion-Based Optical Sensors for Multimodal Strain Measurement in Soft Devices," *IEEE Sensors Conference,* 2017.